Macromolecules

pubs.acs.org/Macromolecules Article

Tailoring Rate and Temperature-Dependent Fracture of Polyether Networks with Organoaluminum Catalysts

Aaliyah Z. Dookhith, Nathaniel A. Lynd, and Gabriel E. Sanoja*

Cite This: *Macromolecules* 2023, 56, 40−48 Read Online

ACCESS | Metrics & More | Article Recommendations | Supporting Information

ABSTRACT: Polyethers are ubiquitous in engineering and biomedical applications because their oxygen-rich backbone allows them to interact with a variety of polar small molecules such as ions, gases, and pharmaceuticals. These materials are also able to sustain large reversible deformations when cross-linked at the molecular scale, leading to an interesting combination of functional and mechanical properties. We synthesized two families of polyether networks by organoaluminum-catalyzed ring-opening copolymerization of ethyl glycidyl ether (EGE) monomer and 1,4-butanediol diglycidyl ether (BDGE) cross-linker and explored the relationship between network architecture and fracture properties. The key result is that living copolymerizations, as enabled by a chelate of triethylaluminum with dimethylaminoethanol, afford access to a critical cross-link density, $\nu_x \approx 3 \times 10^{25}$ chains/m^3, and loss tangent, tan(δ) ≈ 0.09, at which fracture is dominated by chain scission rather than friction. Such control over the fracture resistance of polyether networks unveils the potential of living copolymerizations to design the functional and mechanical properties of soft materials.

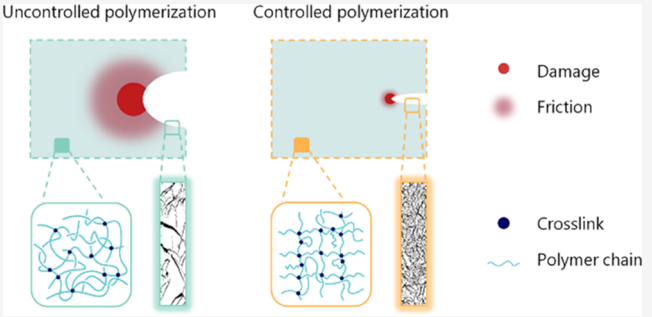

INTRODUCTION

Polyethers constitute an interesting class of materials for polymer electrolytes, membranes, and drug delivery applications because their oxygen-rich backbone allows them to interact with a variety of polar small molecules like ions[1,2] and pharmaceuticals.[3] Although these materials can be readily synthesized from epoxide monomers, they remain rather unexplored due to the low conversions and extended reaction times inherent to many epoxide ring-opening polymerizations. As a result, polyethers are primarily used as low molecular weight polyol precursors of polyurethane rubbers or as non-ionic triblock copolymer surfactants.[4]

Efforts to synthesize high molecular weight polyethers date to the anionic polymerization of ethylene oxide by Staudinger in the 1930s, with one of the most noteworthy contributions being that of Vandenberg in the 1950s.[5,6] By serendipitously combining triethylaluminum ($AlEt_3$), water, and acetyl acetone, Vandenberg synthesized an organoaluminum catalyst that regioselectively polymerizes monomers like propylene oxide and epichlorohydrin to high molecular weight. This catalyst affords polar elastomers of outstanding fuel resistance, but its obscure active species precludes control over the kinetics of epoxide ring-opening polymerization and polymer molecular weight. More recently, Lynd and co-workers synthesized chelates of trialkylaluminum (AlR_3) with dialkylaminoethanol to attain control over the kinetics of polymerization, enabling synthesis of polyethers of narrow dispersity, well-defined molecular weight, and tailored end-group functionality. However, it is worth noting that Naumann,[7,8] Deffieux,[9] Coates,[10,11] and others[12] have attained similar control using a range of catalysts.

Despite major progress in controlling the synthesis of high molecular weight polyethers, not much attention has been paid to the synthesis of polyether networks. These materials are three-dimensional (3D) arrangements of polymer chains interconnected at cross-linking points and, thus, exhibit rubber-like mechanical properties.[13] Long-established molecular models on properties like elasticity, swelling, and fracture idealize networks as homogeneous arrangements of polymer chains when, in reality, they are heterogeneous and pervaded by topological defects that affect the bulk mechanical properties.[14] As such, numerous investigations have focused on controlling the architecture of polymer networks by cross-linking polymer chains of narrow dispersity, well-defined molecular weight, and suitable end-group functionality.[15−18] However, these materials are often synthesized by copolymerizing a monomer and cross-linker: a strategy with a more elusive relationship between synthetic conditions, network

Received: September 21, 2022
Revised: December 9, 2022
Published: December 27, 2022

https://doi.org/10.1021/acs.macromol.2c01955
Macromolecules 2023, 56, 40−48

architecture, and mechanical properties. Fukuda,[19,20] Billingham and Armes,[21,22] Matyjaszewski,[23−25] and co-workers have argued, for example, that networks synthesized by controlled radical copolymerization of vinyl monomers and cross-linkers (e.g., acrylates, methacrylates, and styrenes) are presumably more homogeneous than those synthesized by free radical copolymerization due to the reversible activation and deactivation of polymer chain ends during gelation. Yet, how such control over the network architecture ultimately affects the bulk mechanical properties, particularly at large deformations, remains unknown.

We recently started to address this question by investigating the role of organoaluminum catalysts on the architecture and mechanical properties of polyether networks.[26] Using networks derived from the ring-opening copolymerization of ethyl glycidyl ether (EGE) monomer and 1,4-butanediol diglycidyl ether (BDGE) cross-linker, we demonstrated that, at similar catalyst loadings, the Vandenberg catalyst yields loosely cross-linked, entangled, soft, and extensible networks, whereas the Lynd catalyst, instead, affords highly cross-linked, stiff, and brittle networks. Such catalytic control over the network architecture serves as a strategy to rationally design the mechanical properties of polyethers but also raises a question on what the role of usage conditions like rate and temperature is on their fracture.

Here, we examine this question by undertaking a fracture mechanics approach, where failure results from the propagation of a preexisting crack when the applied energy release rate, G, overcomes the fracture energy, G_c. By evaluating the mechanical properties of poly(ethyl glycidyl ether) networks synthesized either with the Vandenberg or the Lynd catalyst over a range of temperatures and stretch rates, we construct master curves for the fracture energy, G_c, as a function of the reduced crack propagation velocity, $a_T v$. Our results indicate that there is a critical cross-linking density at which the fracture energy, G_c, transitions from a damage- to a friction-dominated regime, highlighting the potential of organoaluminum catalysts and other living copolymerizations to fine-tune the mechanical properties of polymer networks.

BACKGROUND

In the realm of solid mechanics, fracture results from the propagation of a preexisting crack at a critical energy release rate, $G \approx G_c$. This approach was pioneered by Rivlin and Thomas in their seminal work on rubbers[27] and describes the fracture energy, G_c, as

$$G_c = G_0(1 + \phi(a_T v)) \tag{1}$$

where $\phi(a_T v)$ is a velocity-dependent dissipative factor and G_0 is an intrinsic or threshold fracture energy. The physics underlying this equation is rather simple: the amount of energy required to propagate a crack is that dissipated by the material through mechanisms like damage and friction. Eq 1 successfully describes the G_c of a range of elastomers and hydrogels,[18,28−30] but it does not provide any insight on the role of network architecture on the fracture properties.

Lake and Thomas addressed this issue by molecularly modeling the strength of highly elastic materials as[31]

$$G_0 = \Sigma_x N_x U_b \tag{2}$$

In this equation, G_0 is the threshold fracture energy, Σ_x is the areal density of elastically active polymer chains, N_x is the number of covalent bonds between cross-links, and U_b is the energy of a covalent bond (i.e., typically the energy of a C−C bond ≈350 kJ/mol but recently revised by Craig and co-workers to ≈60 kJ/mol based on a probabilistic view of bond scission[32]). Namely, the Lake and Thomas model assumes that the minimum amount of energy required to propagate a crack corresponds to the energy stored in a monolayer of stretched polymer chains. For an ideal polymer network, however, Σ_x and N_x are coupled through

$$\Sigma_x = \frac{\nu_x \langle R_0 \rangle^{1/2}}{2} \approx \frac{\nu_x (C_\infty N_x)^{1/2} l_0}{2} \tag{3}$$

where $\langle R_0 \rangle^{1/2}$ is the average end-to-end distance of an elastic polymer chain, C_∞ the characteristic ratio, and l_0 is the length of a covalent bond along the polymer backbone. Hence, the threshold fracture energy, G_0, is related to the density of elastic chains, ν_x, by

$$G_0 = U_b N_x \frac{\nu_x (C_\infty N_x)^{1/2} l_0}{2} \approx \frac{U_b l_0 C_\infty{}^{1/2}}{2} \left(\frac{\rho N_A}{M_0}\right)^{3/2} \nu_x{}^{-1/2} \tag{4}$$

Here, ρ, M_0, and N_A are, respectively, the density of the polymer network, the molar mass of the monomer, and Avogadro's number. Equation 4 unveils the familiar trade-off between stiffness and toughness in polymer networks, an observation that has been experimentally verified in materials that do not dissipate much energy by friction such as elastomers at high temperatures[33] and hydrogels with high water content.[34] More recently, the Lake and Thomas model has been revised by Arora et al.,[35] Lin et al.,[36] and Barney et al.[37] to account for the role of topological defects on the threshold fracture energy, G_0. Yet, polymer networks are often used under conditions where the fracture energy, G_c, is dominated by friction, $\phi(a_T v) \gg 1$, raising the question of what the effect of entanglements and other topological defects is on energy dissipation and fracture.

Molecular friction is important for fracture when crack propagation occurs on time scales comparable to those of polymer chain relaxation. However, given that the dynamics of polymer chains are generally governed by multiple relaxation times, the contribution of molecular friction to the fracture energy, G_c, is complex and typically evaluated using an empirical approach based on linear viscoelasticity, where the velocity-dependent dissipative factor, $\phi(a_T v)$, is given by

$$\phi(a_T v) \sim (a_T v)^n \tag{6}$$

Here, a_T is the Williams−Landel−Ferry shift factor, v is the crack propagation velocity, and n is a power-law exponent that measures the contribution of molecular friction to energy dissipation and fracture. Numerous investigations have used this approach to study the effects of temperature and stretch rate on the fracture energy, G_c, noteworthy ones being that of Gent and co-workers on styrene-butadiene rubber $n \approx 0.4$,[28] that of Gong and co-workers on double-network hydrogels $n \approx 0.2$,[29] and, of particular interest to our work, that of Creton and co-workers on polyurethanes synthesized by end-linking low molecular weight polyols with trifunctional isocyanates.[18] In this latter work, n notably depends on the dispersity of the precursor chains, highlighting the importance of network architecture on the fracture properties of polymer networks.

https://doi.org/10.1021/acs.macromol.2c01955
Macromolecules 2023, 56, 40−48

RESULTS AND DISCUSSION

We synthesized a series of polyether networks through epoxide ring-opening copolymerization of ethyl glycidyl ether (EGE) monomer and 1,4-butanediol diglycidyl ether (BDGE) cross-linker. Detailed synthetic conditions are provided in the Materials and Methods section and Table S3 of Dookhith et al.,[26] but they differ both in the choice of organoaluminum catalyst (Figure 1A) and nominal cross-linker concentration.

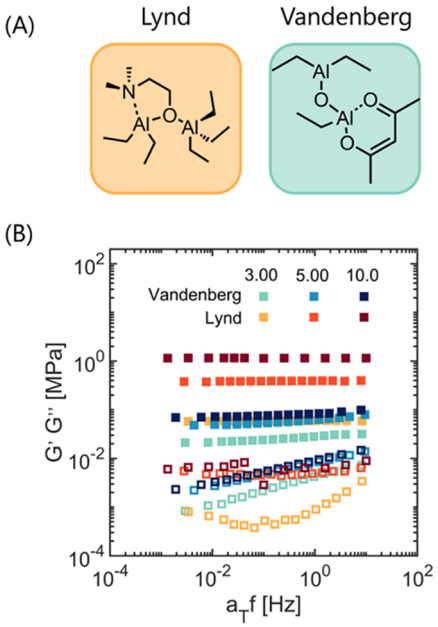

Figure 1. (A) Stoichiometrically representative structures of the Lynd and Vandenberg catalysts. (B) Linear viscoelastic properties of PEGE networks. Storage (■) and loss (□) moduli, G' and G'', indicate that networks synthesized with the Vandenberg catalyst are softer and more viscoelastic than those synthesized with the Lynd catalyst. Figure reproduced from Dookhith et al.[26]

These networks are analogous to those synthesized by Dookhith et al.,[26] and their densities of chemical cross-links and entanglements are summarized in Table 1. The key result from this work was that organoaluminum catalysts provide control over the architecture and mechanical properties of the gel fraction of polyether networks (i.e., after extracting the sol fraction with organic solvent and drying under vacuum). The Vandenberg catalyst afforded loosely cross-linked, entangled, soft, and extensible networks, whereas the Lynd catalyst, instead, led to highly cross-linked, stiff, and brittle networks. This trade-off between stiffness and elasticity at low deformations (i.e., high modulus and negligible energy dissipation) and resistance to crack propagation (i.e., toughness) is characteristic of polymer networks that rely on molecular friction to dissipate energy in the vicinity of the crack tip and is further investigated in this work. For nomenclature purposes, we refer to these networks as Vandenberg- and Lynd-catalyzed networks, though it is worth noting that, strictly speaking, these organoaluminum catalysts were used to copolymerize EGE and BDGE rather than catalyze the networks themselves.

A typical measure of the linear viscoelastic properties is the complex storage and loss moduli, G' and G'', and this is reproduced from Dookhith et al. in Figure 1B.[26] Vandenberg-catalyzed networks exhibit $G' \approx 0.1$ MPa at 1 Hz, frequency-dependent G'', and $G' \gg G''$, whereas Lynd-catalyzed networks, instead, exhibit $G' \approx 1$ MPa at 1 Hz and a rubbery plateau. The exception is the Lynd-catalyzed network synthesized with 3 mol % BDGE, which has a minimum in G'' at 0.1 Hz. Overall, these complex moduli reveal two important features. The first is that Vandenberg-catalyzed networks are soft and viscoelastic irrespective of the cross-linker concentration, and the second is that Lynd-catalyzed networks become stiffer and more elastic as the nominal cross-linker concentration, x, progressively increases from 3 to 10 mol %. Such differences in the viscoelastic properties affect energy dissipation and fracture as will be subsequently discussed.

To probe the effect of temperature and stretch rate on the mechanical properties of PEGE networks, we subjected them to uniaxial elongation until failure and single-edge notch crack propagation. Representative stress−stretch curves for the networks synthesized with 5 mol % BDGE are presented in Figure 2A,B (see others in Figures S1 and S2), and these demonstrate, once again, the significant control afforded by organoaluminum catalysts over mechanical properties like stiffness, extensibility, and toughness. Such stress−stretch curves can be used to estimate the fracture energy, G_c, using Greensmith's approximation[38]

$$G_c = \frac{6c_0}{\sqrt{\lambda_c}} W(\lambda_c) \tag{7}$$

In this equation, c_0 is the initial crack length, λ_c is the critical stretch for crack propagation, and $W(\lambda_c)$ is the strain energy density of an unnotched specimen uniaxially stretched to λ_c. Results are summarized in Figure 2C,D and unveil that both families of networks are tougher at low temperature and high stretch rate or, namely, that molecular friction is indeed important for energy dissipation and fracture.

We further evaluated the contribution of molecular friction to the fracture energy, G_c, using an empirical approach based on linear viscoelasticity (eq 6), where the crack propagation

Table 1. Composition and Mechanical Properties of PEGE Networks[a]

catalyst	x (mol %)	E (MPa)	G_c (J/m^2)	ν_x (10^{24} m^{-3})	ν_e (10^{24} m^{-3})	n
Lynd	3	0.8	57	51	18	0.4
	5	2.0	21	160	8	0.2
	10	4.3	13	470	0	0.1
Vandenberg	3	0.3	106	22	5	0.6
	5	0.3	80	24	11	0.6
	10	0.3	63	25	5	0.6

[a]Nominal concentration of BDGE cross-linker during gelation, x, Young's modulus, E, at 30 °C, fracture energy, G_c, at 30 °C, viscoelastic exponent, n, and densities of chemical cross-links, ν_x, and entanglements, ν_e, at 30 °C.

https://doi.org/10.1021/acs.macromol.2c01955
Macromolecules 2023, 56, 40−48

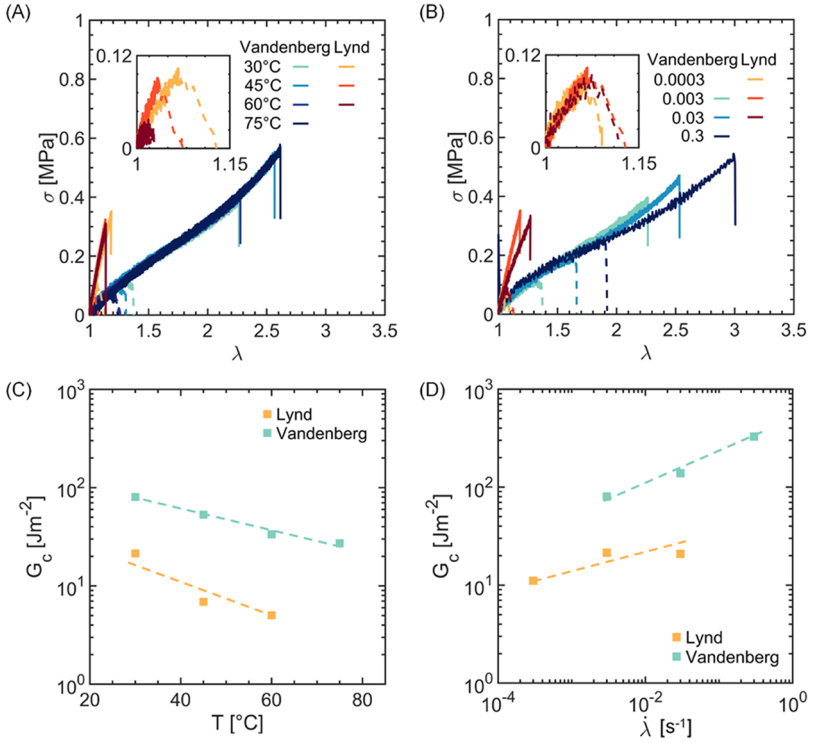

Figure 2. Mechanical properties of PEGE networks cross-linked with 5 mol % BDGE. Stress−stretch curves over a range of (A) temperatures at an initial stretch rate of 0.003 s^{-1} and (B) stretch rates at a temperature of 30 °C for notched (dashed) and unnotched (solid) specimens. Estimates of the fracture energy, G_c, over a range of (C) temperatures and (D) stretch rates reveal the importance of viscoelasticity on energy dissipation and fracture.

velocity, v, is shifted by the Williams−Landel−Ferry (WLF) factors, a_T. Results are summarized in Figure 3 and Table 1

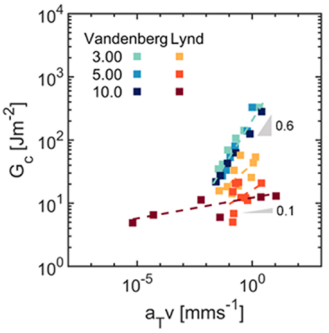

Figure 3. Rate- and temperature-dependent fracture of PEGE networks as given by the fracture energy, G_c, as a function of the rescaled crack velocity, $a_T v$.

(see details in Figures S8−S11 and Table S1) and demonstrate the leverage afforded by the organoaluminum catalysts and the nominal concentration of cross-linker over the fracture properties. Vandenberg-catalyzed networks collapse onto a master curve with power-law exponent, $n \approx 0.6$, whereas Lynd-catalyzed networks, instead, transition from viscoelastic, $n \approx 0.4$, to elastic, $n \approx 0.1$, fracture as the cross-linker concentration progressively increases. These power-law exponents are comparable to those of viscoelastic styrene-butadiene rubber (SBR), $n \approx 0.4$, and natural rubber (NR), $n \approx 0.1$, though the latter is insensitive to rate and temperature due to strain-induced crystallization.[39] Particularly noteworthy is the fracture behavior of the Lynd-catalyzed network synthesized with 5 mol % BDGE, $n \approx 0.2$, as this material appears near-perfectly elastic in its response to linear amplitude oscillatory shear (see plateau modulus in Figure 1B) despite being rather viscoelastic when subject to monotonic crack propagation. This observation indicates that the fracture properties are not necessarily controlled by the mechanical response at low deformations, but, instead, by that at large deformations as experienced in the vicinity of the crack tip.

The size of the large deformation zone, often referred to as a process zone, can be estimated from the elasto-fracture length, $\varepsilon_L \sim G_c/E$, as discussed by Qi et al. in their seminal investigation on silicone elastomers[40] or by Long et al. and Creton et al. in recent reviews.[41,42] This length scale typically scales with the crack tip opening displacement, $\delta_{COD} \sim \varepsilon_L^{\alpha}$, with the exponent α being near one ($\alpha \approx 1$) in a range of soft materials. Figure 4A reveals that such scaling relation, $\delta_{COD} \sim \varepsilon_L$, is valid for networks synthesized with the Vandenberg catalyst, but not for those synthesized with the Lynd catalyst where $\alpha \approx 0.6$. Hence, synthesizing polyether networks by controlled copolymerization notably compromises crack blunting before propagation, leading to numerous bifurcations at the crack tip as well as rough fracture surfaces (Figure 4B). This behavior is qualitatively similar to that reported by Barney et al. in poly(ethylene glycol) hydrogels subjected to needle-induced cavitation, where the ratio of the elasto-fracture length, ε_L, to the crack geometry (i.e., cavity radius) controls the transition from smooth inflation to rough fracture.[43] Our estimates of the surface roughness, R, from the areal density of black pixels in binarized SEM images indicate that this transition from rough to smooth fracture occurs as $\varepsilon_L/\delta_{COD} \rightarrow 1$, suggesting that it is a mesoscopic manifestation of the

https://doi.org/10.1021/acs.macromol.2c01955
Macromolecules 2023, 56, 40−48

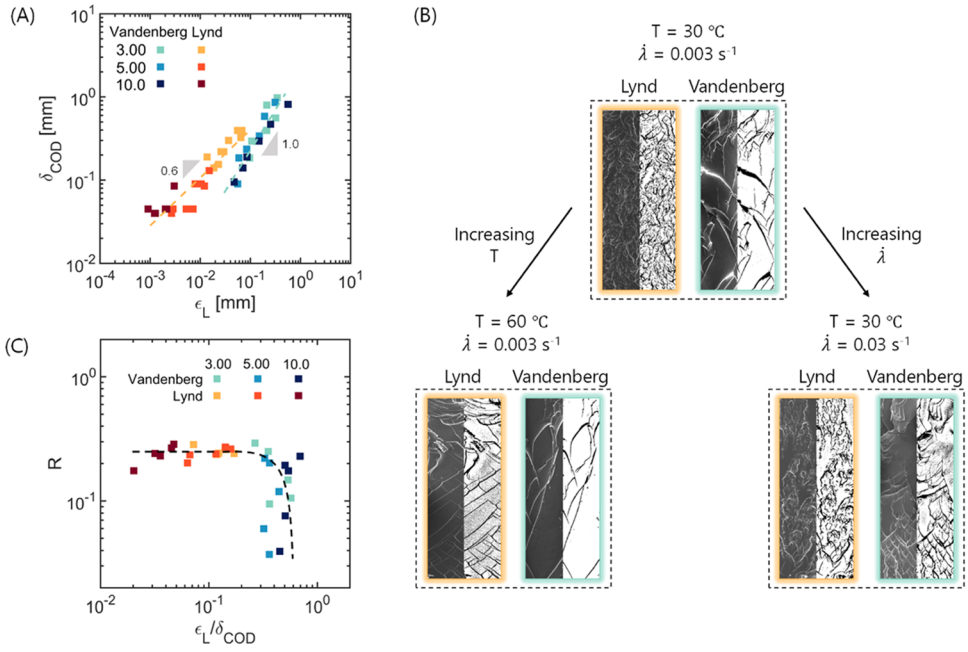

Figure 4. Mesoscopic picture of fracture in PEGE networks. (A) Scaling of the crack tip opening displacement, δ_{COD}, with the elasto-fracture length, ε_L. (B) SEM images of the fracture surfaces after crack propagation. (C) Surface roughness, R, as a function of $\varepsilon_L/\delta_{COD}$: the ratio of the characteristic length scale of the process zone to that of the crack geometry.

different network architectures attained with the Lynd and Vandenberg catalysts (see details in Figures S15−S17).

So far, we have established a connection between the macroscopic fracture energy, G_c, and the mesoscopic region ahead of the crack tip, ε_L, neglecting features of the network architecture such as chemical cross-links, entanglements, and topological defects. To examine the role of such features on the fracture of polyether networks, we considered the stress−stretch curves in Figure 2A,B (and Figures S1 and S2) within the molecular model of Rubinstein and Panyukov,[44] where the engineering stress in uniaxial tension, σ_N, is given by

$$\sigma_N = \left(\nu_x + \frac{\nu_e}{0.74\lambda + 0.61\lambda^{-0.5} - 0.35}\right) k_B T \left(\lambda - \frac{1}{\lambda^2}\right) \quad (8)$$

In this equation, λ is the stretch, and ν_x and ν_e are the respective densities of chemical cross-links and entanglements in the undeformed configuration. The Rubinstein−Panyukov model describes the mechanical response of entangled polymer networks up to the stress softening regime where the polymer chains are stretched far from their limiting extensibility, λ_l, as is the case for most of our polyether networks when subject to low or moderate deformations ($\lambda < 2.2$). The exception is the network synthesized with the Lynd catalyst at 10 mol % BDGE cross-linker, which has $\lambda_l \approx 1.5$ and a stretch at break $\lambda_b \approx 1.1$. Acknowledging this limitation, we conducted nonlinear least-square regressions to estimate ν_x and ν_e for both families of networks. Results are summarized in Table 1 (see details in Figures S3−S7) and indicate that, irrespective of the temperature and the stretch rate, networks synthesized with the Vandenberg catalyst are less cross-linked and more entangled than those synthesized with the Lynd catalyst. This difference in network architecture is probably related to the kinetics of copolymerization during gelation, though this hypothesis requires further experimental validation.

An important result that emerges from the Rubinstein−Panyukov fits is that inefficient cross-linking and entanglements lead to energy dissipation and toughness. This effect is also observed when considering the fracture energy, G_c, within the molecular model of Lake and Thomas on the strength of highly elastic materials (eq 7),[31] where $G_c \sim \nu_x^{-1/2}$. Results are presented in Figure 5A and unveil that networks synthesized with the Lynd catalyst obey the Lake and Thomas scaling, whereas networks synthesized with the Vandenberg catalyst, instead, notably deviate from it with $G_c \sim \nu_x^{-4}$. A similar observation was reported by Dookhith et al. for fracture of analogous PEGE networks at room temperature and an initial stretch rate of 0.003 s^{-1},[26] and here, we simply generalize the result for a range of temperatures and stretch rates. However, we provide additional insight by normalizing the rescaled crack propagation velocity, $a_T v$, by the elasto-fracture length, ε_L. Whether this length scale is the relevant one for describing crack propagation in viscoelastic solids remains a topic of active investigation,[45,46] yet we use it here to estimate a characteristic timescale of fracture by crack propagation, $a_T v/\varepsilon_L$. Results are summarized in Figure S13 and convey a similar picture to that presented in Figure 3 and Table 1: a transition from viscoelastic to elastic fracture as the cross-linker concentration progressively increases.

This characteristic timescale (or frequency) of fracture by crack propagation, $a_T v/\varepsilon_L$, can now be used to estimate the contribution of molecular friction to energy dissipation, evaluating loss tangent, $\tan(\delta)$, under linear amplitude oscillatory shear (Figure 1B) at $a_T f \approx a_T v/\varepsilon_L$. Results are summarized in Figure 5B and enable construction of a multiscale picture of fracture. At low cross-linking densities, ν_x, the networks are pervaded by entanglements and other topological defects with sufficient mobility to slide against each other, dissipate energy by friction, and fracture with a rate and temperature dependence. As the cross-linking density increases, $\nu_x \approx 3 \times 10^{25}$ chains/m^3, and loss tangent decreases, $\tan(\delta) \approx 0.09$, the networks still contain some entanglements and topological defects that slide against each other, but

https://doi.org/10.1021/acs.macromol.2c01955
Macromolecules 2023, 56, 40−48

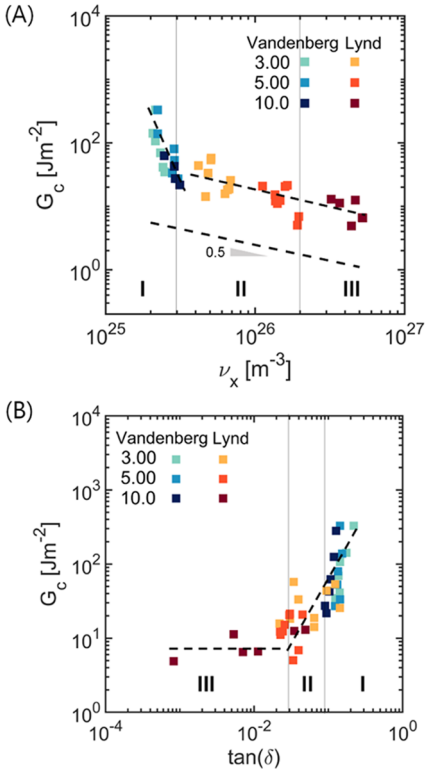

Figure 5. Contributions of friction and damage to the fracture energy of PEGE networks. (A) Fracture energy, G_c, of Lynd-catalyzed networks scales with the prediction of Lake and Thomas, $G_c \sim \nu_x^{-0.5}$, suggesting that energy dissipation is primarily by network chain scission (i.e., damage). (B) Fracture energy, G_c, becomes rate- and temperature-dependent at a critical tan(δ) ≈ 0.03, indicating that at cross-link densities, ν_x, ranging from 3×10^{25} to 2×10^{26} chains/m^3 PEGE networks are viscoelastic in fracture despite dissipating energy mainly by network chain scission.

dissipation is mainly by damage. After all, the fracture energy, G_c, in this regime still scales as predicted by the Lake and Thomas model, $G_c \sim \nu_x^{-1/2}$, which neglects contributions of chain friction to energy dissipation. Finally, at a cross-linking density, $\nu_x \approx 2 \times 10^{26}$ chains/m^3, and loss tangent, tan(δ) ≈ 0.03, the entanglements and topological defects freeze or become kinetically arrested, leading to energy dissipation primarily by damage and near-perfect elasticity in fracture, $n \approx 0.1$. A depiction of this transition from viscoelastic to elastic fracture is presented in Scheme 1.

CONCLUDING REMARKS

Polyether networks synthesized by epoxide ring-opening copolymerization of monomer and cross-linker exhibit architecture and mechanical properties that notably depend on the choice of organoaluminum catalyst and the nominal concentration of cross-linker. Vandenberg-catalyzed networks are loosely cross-linked and pervaded by entanglements irrespective of the nominal cross-linker concentration, resulting in notable dissipation by molecular friction, process zones ca. 0.1−1 mm, smooth fracture surfaces, and viscoelastic fracture. Lynd-catalyzed networks, instead, are highly cross-linked and contain some entanglements that get kinetically arrested at a critical cross-linker concentration, resulting in notable dissipation by molecular damage, process zones ca. 1−10 μm, rough fracture surfaces, and a transition from viscoelastic to elastic fracture at high cross-linker concentrations. Such control over the architecture and fracture properties of polyether networks is a consequence of the copolymerization livingness procured by the Lynd catalyst, a chelate of triethylaluminum with dimethylaminoethanol, during gelation.

Molecular models that describe the nonlinear elastic response and fracture energy of polymer networks serve to draw relationships between the network architecture and fracture properties but have some unresolved limitations that are worth noting. First, the Rubinstein−Panyukov model assumes that polymer networks are composed of an ensemble of polymer chains topologically constrained by a mean field in the undeformed state.[44] This description is rather accurate at low to moderate deformations where the chains adopt a Gaussian configuration but less so in the process zone where the chains are stretched near their limiting extensibility. In this regard, efforts that combine theory and experiments to understand the load-bearing capacity of polymer chains within the process zone are of utmost importance. Second, the Lake and Thomas model only considers dissipation by scission of a

Scheme 1. Multi-Scale Picture of Fracture of PEGE Networks Illustrating a Transition from a Friction- (I) to a Damage-Dominated (III) Regime

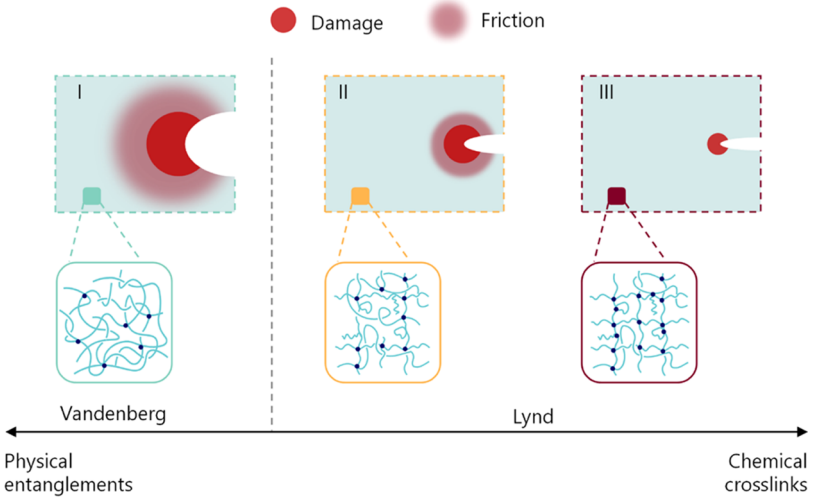

https://doi.org/10.1021/acs.macromol.2c01955
Macromolecules 2023, 56, 40−48

monolayer of elastic polymer chains and neglects the contributions of chain friction to the fracture energy.[31] These assumptions are inaccurate and outline a grand challenge in the field of soft matter physics: understanding and predicting the strong coupling between macroscopic properties like the fracture energy, G_c, and the local processes like damage and friction that occur in the vicinity of the crack tip.

Finally, polyether networks synthesized by epoxide ring-opening copolymerization of the monomer and cross-linker are unfilled, meaning that they are tougher at low temperatures and high stretch rates despite being, in more absolute terms, brittle with $G_c \sim 10-100$ J/m^2. These materials would typically be used notably above the glass transition temperature, T_g, to avoid viscoelastic losses and heating or, namely, in a rubbery regime where the loss tangent, $\tan(\delta)$, at a representative timescale of deformation is well below 0.1 and dissipation by chain friction is negligible. Future work should focus on toughening these soft, elastic, and functional materials through network design.

MATERIALS AND METHODS

Materials. Unless otherwise specified, all chemicals were used as received. Ethyl glycidyl ether (EGE), 1,4-butanediol diglycidyl ether (BDGE), and 2.0 M butyl magnesium chloride in THF were sourced from TCI; acetyl acetone, anhydrous diethyl ether, 1.0 M triethylaluminum ($AlEt_3$) in hexanes, and dimethylaminoethanol, from Millipore Sigma; methanol from VWR; and hydrochloric acid from Fischer.

Slippery films of chemical-resistant Teflon PTFE and UHMW Polyethylene were sourced from McMaster-Carr with a thickness of 0.010″.

EGE (100 mL) was purified by stirring over butyl magnesium chloride (2.0 M in THF, 1 mL) for 1 h and distilling under vacuum. Caution! Butyl magnesium chloride is a pyrophoric and moisture-sensitive chemical and should be handled with appropriate care. Distilled EGE, acetyl acetone, and DI water were placed in dry septum-sealed bottles, sparged with N_2 for 45 min, and transferred into a N_2-filled glovebox.

Synthesis of the Vandenberg Catalyst. The Vandenberg catalyst was prepared following a procedure reported by Beckingham et al.[47] and more recently by Dookhith et al.[26] A dry septum-sealed bottle equipped with a Teflon stir bar was placed in a LN_2 cold well located inside a N_2-filled glovebox. Anhydrous diethyl ether (40 mL) and $AlEt_3$ (1.0 M in hexanes, 40 mL, 40 mmol, 2 equiv) were sequentially added with gastight syringes and stirred for 30 min. Caution! $AlEt_3$ is a pyrophoric and moisture-sensitive chemical and should be handled with appropriate care. Then, acetyl acetone (2.04 mL, 20 mmol, 1 equiv) was added with a gastight syringe and the reaction stirred for 2 h. Finally, DI water was added (0.36 mL, 20 mmol, 1 equiv) with a gastight syringe, and the reaction stirred overnight at room temperature.

Synthesis of the Lynd Catalyst. The Lynd catalyst was prepared following a procedure reported by Rodriguez et al.[48] and more recently by Dookhith et al.[26] A dry septum-sealed bottle equipped with a Teflon stir bar was immersed in a LN_2 cold well located inside a N_2-filled glovebox. $AlEt_3$ (1.0 M in hexanes, 12 mL, 12 mmol, 2.5 equiv) and dimethylaminoethanol (0.445 mL, 4.4 mmol, 1 equiv) were sequentially added with syringes, and the reaction stirred overnight allowing the cold well to equilibrate to room temperature.

The Lynd catalyst was purified inside the N_2-filled glovebox, recrystallizing three times from hexanes in the LN_2 cold well to remove excess $AlEt_3$, decanting the solid product, and drying under vacuum overnight at room temperature.

Synthesis of Poly(ethyl glycidyl ether) Networks. Networks were synthesized by bulk copolymerization of EGE and BDGE. In a N_2-filled glovebox, monomer EGE, cross-linker BDGE, and organo-aluminum catalyst (1 mol %) were well mixed in a 20 mL scintillation vial and then transferred to a mold composed of two PTFE- (Lynd) or polyethylene-covered (Vandenberg) glass plates sealed with a silicone rubber spacer (≈0.1 cm thick). Polymerization was conducted in the N_2-filled glovebox antechamber for 6 days at 60 °C, and the resulting polymer networks transferred outside of the glovebox for termination and purification. Typical network dimensions were 8 × 4 × 0.1 cm^3.

Polymer networks were terminated by swelling in a solution of acidic methanol (0.1 M HCl) in DI water (44 mL, 90% v/v) for 2 h, washed in methanol for 2 h (4 × 40 mL), and dried first under ambient conditions for 4 h and then under vacuum at room temperature overnight.

Gel fractions were determined from the mass difference between the as-polymerized and terminated networks and are above 80%. The exception was the network synthesized with the Lynd catalyst at 3 mol % BDGE, which has a gel fraction of 60% (see Table S3 of Dookhith et al.[26])

The aluminum concentrations of purified networks (i.e., of the gel fraction) synthesized with 10 mol % BDGE were determined by ICP-MS and are 7900 ppm (Lynd) and 100 ppm (Vandenberg).

All mechanical characterization was conducted on the gel fraction of the polymer networks.

Rheology. Polymer networks were punch-cut into cylindrical specimens of 8 mm diameter and ≈1 mm thickness, and their rheological properties evaluated in a Discovery HR-2 rheometer equipped with stainless steel flat plates of 8 mm diameter.

Frequency sweeps from 0.1 to 100 rad/s at temperatures from 30 to 75 °C were performed within the linear viscoelastic regime at a strain amplitude of 1.00%. Master curves for the storage and loss moduli were constructed by time-temperature superposition, using a reference temperature of 30 °C and horizontal, a_T, and vertical, b_T, shift factors. The horizontal shift factors, a_T, are summarized in Figure S11, whereas the vertical shift factors, b_T, are approximately one, $b_T \approx 1.0$.

Uniaxial Tension. Polymer networks were punch-cut into dog-bone-shaped specimens of 20 mm gauge length, 4 mm width, and ≈ 1 mm thickness. These were marked with two dots of white paint and deformed with an Instron 34TM5 equipped with a 100 N load cell and a video extensometer. The initial stretch rate ranged from 0.0003 to 0.3 s^{-1} and the temperature from 30 to 75 °C. The resulting force−displacement curves were used to compute the engineering stress, σ_N, and stretch, λ.

Single-Edge-Notch Crack Propagation. Polymer networks were punch-cut into dog-bone-shaped specimens of 20 mm gauge length, 4 mm width, and ≈1 mm thickness. These were cut with a fresh razor blade to introduce a crack of ≈1 mm length, marked with two dots of white paint and deformed with an Instron 34TM5 equipped with a 100 N load cell and a video extensometer. The initial stretch rate ranged from 0.0003 to 0.3 s^{-1} and the temperature from 30 to 75 °C. The resulting force−displacement curves were used to compute the engineering stress, σ_N, and stretch, λ.

Scanning Electron Microscopy. Crack surfaces were imaged using a FEI Quanta 650 ESEM, setting the electron beam to 20 kV, the aperture to 3.0, and the magnification to 31X. Images were binarized in MATLAB using a sensitivity of 0.55 for Lynd- and 0.40 for Vandenberg-catalyzed networks, and the average surface roughness determined from the areal density of the black pixels according to

$$R = \frac{N_1}{N_1 + N_0} \tag{9}$$

where N_1 and N_0 are the numbers of black and white pixels, respectively.

ASSOCIATED CONTENT

Supporting Information

The Supporting Information is available free of charge at https://pubs.acs.org/doi/10.1021/acs.macromol.2c01955.

https://doi.org/10.1021/acs.macromol.2c01955
Macromolecules 2023, 56, 40−48

Stress−stretch curves and estimates of the fracture energy, G_c, evaluation of the stress−stretch curves under the molecular model of Rubinstein−Panyukov on entangled polymer networks, fracture by single-edge-notch crack propagation, SEM images of fracture surfaces, and calculations of the elastic modulus (PDF)

AUTHOR INFORMATION

Corresponding Author

Gabriel E. Sanoja − *McKetta Department of Chemical Engineering, The University of Texas at Austin, Austin, Texas 78712, United States;* orcid.org/0000-0001-5477-2346; Email: gesanoja@che.utexas.edu

Authors

Aaliyah Z. Dookhith − *McKetta Department of Chemical Engineering, The University of Texas at Austin, Austin, Texas 78712, United States;* orcid.org/0000-0003-4219-5515

Nathaniel A. Lynd − *McKetta Department of Chemical Engineering, The University of Texas at Austin, Austin, Texas 78712, United States;* orcid.org/0000-0003-3010-5068

Complete contact information is available at: https://pubs.acs.org/10.1021/acs.macromol.2c01955

Author Contributions

Research was designed by A.Z.D. and G.E.S. Synthesis, mechanical characterization, and SEM imaging were conducted by A.Z.D., and data interpreted by A.Z.D., N.A.L., and G.E.S. The manuscript was written by A.Z.D. and G.E.S. and critically revised by all authors. All authors have given final approval to the final version

Funding

This work was funded by The University of Texas at Austin. N.A.L. acknowledges support for synthesis from the National Science Foundation (CHE-2004167) and the Welch Foundation (F-1904)

Notes

The authors declare no competing financial interest.

All data needed to evaluate the conclusions are present in the paper and/or the Supporting Information, as well as in the Texas Data Repository.

ACKNOWLEDGMENTS

The authors acknowledge the use of shared research facilities supported in part by the Texas Materials Institute, the Center for Dynamics and Control of Materials: an NSF MRSEC (DMR-1720595), and the NSF Nanotechnology Coordinated Infrastructure (ECCS-1542159).

REFERENCES

(1) Lascaud, S.; Perrier, M.; Vallee, A.; Besner, S.; Prud'homme, J.; Armand, M. Phase Diagrams and Conductivity Behavior of Poly-(Ethylene Oxide)-Molten Salt Rubbery Electrolytes. *Macromolecules* **1994**, *27*, 7469−7477.

(2) Gorecki, W.; Jeannin, M.; Belorizky, E.; Roux, C.; Armand, M. Physical Properties of Solid Polymer Electrolyte PEO(LiTFSI) Complexes. *J. Phys.: Condens. Matter* **1995**, *7*, 6823−6832.

(3) Lin, C. C.; Anseth, K. S. PEG Hydrogels for the Controlled Release of Biomolecules in Regenerative Medicine. *Pharm. Res.* **2009**, *26*, 631−643.

(4) Vairon, J.-P.; Spassky, N.Industrial Cationic Polymerizations: An Overview. In *In Cationic Polymerizations*; CRC Press,, 1996; pp 697−782. DOI: 10.1201/9780585400433-10.

(5) Vandenberg, E. J. Epoxide Polymers: Synthesis, Stereochemistry, Structure, and Mechanism. *J. Polym. Sci., Part A-1: Polym. Chem.* **1969**, *7*, 525−567.

(6) Vandenberg, E. J.Catalysis: A Key to Advances in Applied Polymer Science. In *Polymeric Materials Science and Engineering, Proceedings of the ACS Division of Polymeric Materials Science and Engineering*; ACS Publications, 1992; Vol. *64*, pp 2−23 DOI: 10.1021/bk-1992-0496.ch001.

(7) Walther, P.; Krauß, A.; Naumann, S. Lewis Pair Polymerization of Epoxides via Zwitterionic Species as a Route to High-Molar-Mass Polyethers. *Angew. Chem., Int. Ed.* **2019**, *58*, 10737−10741.

(8) Sirin-Sariaslan, A.; Naumann, S. Chiral Diboranes as Catalysts for the Stereoselective Organopolymerization of Epoxides. *Chem. Sci.* **2022**, *13*, 10939−10943.

(9) Labbé, A.; Carlotti, S.; Billouard, C.; Desbois, P.; Deffieux, A. Controlled High-Speed Anionic Polymerization of Propylene Oxide Initiated by Onium Salts in the Presence of Triisobutylaluminum. *Macromolecules* **2007**, *40*, 7842−7847.

(10) Peretti, K. L.; Ajiro, H.; Cohen, C. T.; Lobkovsky, E. B.; Coates, G. W. A Highly Active, Isospecific Cobalt Catalyst for Propylene Oxide Polymerization. *J. Am. Chem. Soc.* **2005**, *127*, 11566−11567.

(11) Widger, P. C. B.; Ahmed, S. M.; Coates, G. W. Exploration of Cocatalyst Effects on a Bimetallic Cobalt Catalyst System: Enhanced Activity and Enantioselectivity in Epoxide Polymerization. *Macromolecules* **2011**, *44*, 5666−5670.

(12) Herzberger, J.; Niederer, K.; Pohlit, H.; Seiwert, J.; Worm, M.; Wurm, F. R.; Frey, H. Polymerization of Ethylene Oxide, Propylene Oxide, and Other Alkylene Oxides: Synthesis, Novel Polymer Architectures, and Bioconjugation. *Chem. Rev.* **2016**, *116*, 2170−2243.

(13) Treloar, L. R. G.*The Physics of Rubber Elasticity*, 3rd ed.; Oxford University Press: Oxford, U.K., 1975.

(14) Zhong, M.; Wang, R.; Kawamoto, K.; Olsen, B. D.; Johnson, J. A. Quantifying the Impact of Molecular Defects on Polymer Network Elasticity. *Science* **2016**, *353*, 1264−1268.

(15) Sakai, T.; Matsunaga, T.; Yamamoto, Y.; Ito, C.; Yoshida, R.; Suzuki, S.; Sasaki, N.; Shibayama, M.; Chung, U. Design and Fabrication of a High-Strength Hydrogel with Ideally Homogeneous Network Structure from Tetrahedron-like Macromonomers. *Macromolecules* **2008**, *41*, 5379−5384.

(16) Yoo, S. H.; Yee, L.; Cohen, C. Effect of Network Structure on the Stress−Strain Behaviour of Endlinked PDMS Elastomers. *Polymer* **2010**, *51*, 1608−1613.

(17) Genesky, G. D.; Cohen, C. Toughness and Fracture Energy of PDMS Bimodal and Trimodal Networks with Widely Separated Precursor Molar Masses. *Polymer* **2010**, *51*, 4152−4159.

(18) Cristiano, A.; Marcellan, A.; Keestra, B. J.; Steeman, P.; Creton, C. Fracture of Model Polyurethane Elastomeric Networks. *J. Polym. Sci., Part B: Polym. Phys.* **2011**, *49*, 355−367.

(19) Ide, N.; Fukuda, T. Nitroxide-Controlled Free-Radical Copolymerization of Vinyl and Divinyl Monomers. Evaluation of Pendant-Vinyl Reactivity. *Macromolecules* **1997**, *30*, 4268−4271.

(20) Ide, N.; Fukuda, T. Nitroxide-Controlled Free-Radical Copolymerization of Vinyl and Divinyl Monomers. 2. Gelation. *Macromolecules* **1999**, *32*, 95−99.

(21) Bannister, I.; Billingham, N. C.; Armes, S. P.; Rannard, S. P.; Findlay, P. Development of Branching in Living Radical Copolymerization of Vinyl and Divinyl Monomers. *Macromolecules* **2006**, *39*, 7483−7492.

(22) Vo, C.-D.; Rosselgong, J.; Armes, S. P.; Billingham, N. C. RAFT Synthesis of Branched Acrylic Copolymers. *Macromolecules* **2007**, *40*, 7119−7125.

(23) Gao, H.; Li, W.; Matyjaszewski, K. Synthesis of Polyacrylate Networks by ATRP: Parameters Influencing Experimental Gel Points. *Macromolecules* **2008**, *41*, 2335−2340.

(24) Gao, H.; Miasnikova, A.; Matyjaszewski, K. Effect of Cross-Linker Reactivity on Experimental Gel Points during ATRcP of Monomer and Cross-Linker. *Macromolecules* **2008**, *41*, 7843−7849.
(25) Gao, H.; Matyjaszewski, K. Synthesis of Functional Polymers with Controlled Architecture by CRP of Monomers in the Presence of Cross-Linkers: From Stars to Gels. *Prog. Polym. Sci.* **2009**, *34*, 317−350.
(26) Dookhith, A. Z.; Lynd, N. A.; Creton, C.; Sanoja, G. E. Controlling Architecture and Mechanical Properties of Polyether Networks with Organoaluminum Catalysts. *Macromolecules* **2022**, *55*, 5601−5609.
(27) Rivlin, R. S.; Thomas, A. G.Rupture of Rubber. I. Characteristic Energy for Tearing. In *Collected Papers of R.S. Rivlin*; Springer New York: New York, NY, 1997; Vol. *X*, pp 2615−2642. DOI: 10.1007/978-1-4612-2416-7_180.
(28) Gent, A. N.; Lai, S.-M.; Nah, C.; Wang, C. Viscoelastic Effects in Cutting and Tearing Rubber. *Rubber Chem. Technol.* **1994**, *67*, 610−618.
(29) Tanaka, Y.; Kuwabara, R.; Na, Y.-H.; Kurokawa, T.; Gong, J. P.; Osada, Y. Determination of Fracture Energy of High Strength Double Network Hydrogels. *J. Phys. Chem. B* **2005**, *109*, 11559−11562.
(30) Baumberger, T.; Caroli, C.; Martina, D. Fracture of a Biopolymer Gel as a Viscoplastic Disentanglement Process. *Eur. Phys. J. E* **2006**, *21*, 81−89.
(31) Lake, G. J.; Thomas, A. G. The Strength of Highly Elastic Materials. *Proc. R. Soc. London, Ser. A* **1967**, *300*, 108−119.
(32) Wang, S.; Panyukov, S.; Rubinstein, M.; Craig, S. L. Quantitative Adjustment to the Molecular Energy Parameter in the Lake−Thomas Theory of Polymer Fracture Energy. *Macromolecules* **2019**, *52*, 2772−2777.
(33) Bhowmick, A. K. Threshold Fracture of Elastomers. *J. Macromol. Sci., Part C: Polym. Rev.* **1988**, *28*, 339−370.
(34) Akagi, Y.; Sakurai, H.; Gong, J. P.; Chung, U.; Sakai, T. Fracture Energy of Polymer Gels with Controlled Network Structures. *J. Chem. Phys.* **2013**, *139*, No. 144905.
(35) Arora, A.; Lin, T.-S.; Beech, H. K.; Mochigase, H.; Wang, R.; Olsen, B. D. Fracture of Polymer Networks Containing Topological Defects. *Macromolecules* **2020**, *53*, 7346−7355.
(36) Lin, S.; Ni, J.; Zheng, D.; Zhao, X. Fracture and Fatigue of Ideal Polymer Networks. *Extrem. Mech. Lett.* **2021**, *48*, No. 101399.
(37) Barney, C. W.; Ye, Z.; Sacligil, I.; McLeod, K. R.; Zhang, H.; Tew, G. N.; Riggleman, R. A.; Crosby, A. J. Fracture of Model End-Linked Networks. *Proc. Natl. Acad. Sci. U.S.A.* **2022**, *119*, 2−7.
(38) Greensmith, H. W. Rupture of Rubber. X. The Change in Stored Energy on Making a Small Cut in a Test Piece Held in Simple Extension. *J. Appl. Polym. Sci.* **1963**, *7*, 993−1002.
(39) Gent, A. N.Engineering with Rubber. In *Engineering with Rubber*; Carl Hanser Verlag GmbH &: Co. KG: München, 2012; pp I−XVIII. DOI: 10.3139/9783446428713.fm.
(40) Qi, Y.; Zou, Z.; Xiao, J.; Long, R. Mapping the Nonlinear Crack Tip Deformation Field in Soft Elastomer with a Particle Tracking Method. *J. Mech. Phys. Solids* **2019**, *125*, 326−346.
(41) Creton, C.; Ciccotti, M. Fracture and Adhesion of Soft Materials: A Review. *Rep. Prog. Phys.* **2016**, *79*, No. 046601.
(42) Long, R.; Hui, C.-Y.; Gong, J. P.; Bouchbinder, E. The Fracture of Highly Deformable Soft Materials: A Tale of Two Length Scales. *Annu. Rev. Condens. Matter Phys.* **2021**, *12*, 71−94.
(43) Barney, C. W.; Sacligil, I.; Tew, G. N.; Crosby, A. J. Linking Cavitation and Fracture to Molecular Scale Structural Damage of Model Networks. *Soft Matter* **2022**, *18*, 4220−4226.
(44) Rubinstein, M.; Panyukov, S. Elasticity of Polymer Networks. *Macromolecules* **2002**, *35*, 6670−6686.
(45) Hui, C.-Y.; Zhu, B.; Long, R. Steady State Crack Growth in Viscoelastic Solids: A Comparative Study. *J. Mech. Phys. Solids* **2022**, *159*, No. 104748.
(46) Guo, J.; Zehnder, A. T.; Creton, C.; Hui, C.-Y. Time Dependent Fracture of Soft Materials: Linear versus Nonlinear Viscoelasticity. *Soft Matter* **2020**, *16*, 6163−6179.
(47) Beckingham, B. S.; Sanoja, G. E.; Lynd, N. A. Simple and Accurate Determination of Reactivity Ratios Using a Nonterminal Model of Chain Copolymerization. *Macromolecules* **2015**, *48*, 6922−6930.
(48) Rodriguez, C. G.; Ferrier, R. C.; Helenic, A.; Lynd, N. A. Ring-Opening Polymerization of Epoxides: Facile Pathway to Functional Polyethers via a Versatile Organoaluminum Initiator. *Macromolecules* **2017**, *50*, 3121−3130.

https://doi.org/10.1021/acs.macromol.2c01955
Macromolecules 2023, 56, 40−48